Journal of Virology

Virology | Full-Length Text

Interaction of species A rotavirus VP4 with the cellular proteins vimentin and actin related protein 2 discovered by a proximity interactome assay

Pengfei Hao,[1,2] Qiaoqiao Qu,[2] Zhaoxia Pang,[2] Letian Li,[2] Shouwen Du,[2] Limin Shang,[3] Chaozhi Jin,[3] Wang Xu,[2] Zhuo Ha,[2] Yuhang Jiang,[2] Jing Chen,[1,2] Zihan Gao,[2] Ningyi Jin,[1,2] Jian Wang,[3] Chang Li[2]

AUTHOR AFFILIATIONS See affiliation list on p. 15.

ABSTRACT Rotavirus (RV) is one of the most significant pathogens in humans and animals with diarrhea worldwide. Cell entry is the first step in viral infection, and the outer capsid protein VP4 is crucial for RV attachment and internalization. In order to discover novel candidate host factors involved in RV cell entry, a proximity labeling method was applied to systematically investigate the VP4 and host protein interactions. A total of 174 high-confidence host proteins were identified using proximity labeling. Further analysis showed that 88 proteins were located in the cytoskeleton, plasma membrane, and extracellular region, which could be involved in RV entry. Importantly, vimentin (VIM) and actin-related protein 2 (ACTR2) were identified to promote RV infection at an early step. The results of co-immunoprecipitation assay showed that VIM or ACTR2 physically interacted with VP4. Blocking VIM or ACTR2 function by silencing with small interfering RNA or inhibition by specific antibodies significantly restricted RV infection. Furthermore, increasing the amounts of VIM or ACTR2 by overexpression from transfected recombinant proteins or incubation with recombinant proteins promoted RV infection. Collectively, this study revealed that RV VP4 interacted with host proteins and demonstrated that interaction with VIM and ACTR2 promoted RV replication, providing valuable resources and potential drug targets for better understanding and treating this disease.

IMPORTANCE Rotavirus (RV) is an important zoonosis virus, which can cause severe diarrhea and extra-intestinal infection. To date, some proteins or carbohydrates have been shown to participate in the attachment or internalization of RV, including HGBAs, Hsc70, and integrins. This study attempted to indicate whether there were other proteins that would participate in the entry of RV; thus, the RV VP4-interacting proteins were identified by proximity labeling. After analysis and verification, it was found that VIM and ACTR2 could significantly promote the proliferation of RV in intestinal cells. Through further viral binding assays after knockdown, antibody blocking, and recombinant protein overexpression, it was revealed that both VIM and ACTR2 could promote RV replication.

KEYWORDS rotavirus, VP4, VIM, ACTR2, viral entry, proximity labeling

Rotavirus (RV), which belongs to *Reoviridae* family, is one of the most important pathogens in humans and animals with diarrhea, especially in infants and children aged under 5 years old (1). RV can be divided into 10 types, and type A, which was discovered in 1973, is the most serious and well-studied pathogen (2).

The entry of RV is a significant research field, which is a complex process and remains elusive (3). As an outermost viral protein of RV, VP4 is crucial for RV entry and tropism

Editor Stacey Schultz-Cherry, St. Jude Children's Research Hospital, Memphis, Tennessee, USA

Address correspondence to Chang Li, lichang78@163.com, Jian Wang, Wangjian@bmi.ac.cn, or Ningyi Jin, ningyik@126.com.

The authors declare no conflict of interest.

See the funding table on p. 16.

Received 5 September 2023
Accepted 9 September 2023
Published 22 November 2023

Copyright © 2023 American Society for Microbiology. All Rights Reserved.

(3, 4). In terms of host cells, some carbohydrates and proteins have been demonstrated to participate in RV entry. To date, histo-blood group antigens were considered as the most important factors for RV attachment (5), and sialic acid (SA) also participates in RV entry for certain strains (6). Additionally, several proteins have been found to participate in attachment or post-attachment. Heat shock cognate protein 70 (HSPA8; also known as HSC70) (7) and certain integrins (8–10) may participate in RV attachment and internalization via clathrin-mediated endocytosis pathway.

To date, compared with other viruses, just a few of RV receptors or attachment factors have been found. Especially, a limited number of systematic studies on VP4 interacting with host proteins were conducted. Thus, there is an urgent need to eliminate the above-mentioned limitations so as to explore novel host proteins that may participate in RV entry.

A proximity labeling method based on a promiscuous biotin ligase gene (TurboID) was developed to covalently label neighbors of a target protein in host protein with biotin within 10 min (11, 12), which has been applied to detect various protein-protein interactions (PPIs), such as virus-host interaction, including severe acute respiratory syndrome coronavirus 2 (SARS-CoV-2) (13), hepatitis B virus (HBV) (14), Lassa virus (LASV) (15), or other fields, such as brain science (16), cardiovascular events (17), botany (18, 19), and parasitology (20–22).

In the present study, proximity labeling was employed to investigate the PPI networks between VP4 of RV and host factors. The VP4 protein was amplified from a type A RV strain isolated from bat samples (23), which has a broad-spectrum cellular infection. Then, a total of 174 high-confidence proximity labeling host proteins were identified, and it was revealed that vimentin (VIM) and actin-related protein 2 (ACTR2) could promote RV infection, including type A RV strains of MYAS33 [bat, G3P(10)], MSLH14 [bat, G3P(3)], Wa [human, G1P1(8)], and SA11 [monkey, G3P(2)], providing valuable resources and potential drug targets for better understanding and treating of this disease.

RESULTS

Global analysis of VP4 protein interactions

To comprehensively identify host factors related to VP4 of RV, the proximity labeling method was used. The gene encoding RV VP4 (Genbank accession number: KF649187.1) protein was amplified from type A RV MYAS33 strain. Cell infection results showed that MYAS33 could infect distinct cell lines, including chicken embryo fibroblast cell line (DF-1), normal human intestinal epithelial cell line (HIEC-6), rat intestinal epithelial cell line (IEC-6), African green monkey kidney cell line (Vero), and intestinal porcine enterocyte cell line (IPEC-J2; Fig. 1B and C), suggesting a broad-spectrum infectious feature of MYAS33 on the cellular level.

Afterward, the VP4 gene was cloned into a mammalian expression vector pcDNA3.1-TurboID. The plasmid was transfected to HEK293T cells and was then labeled with biotin for 10 min. Mass spectrometry (MS) was performed to identify biotinylated proteins or peptides (Fig. 2A), and VP4-interacting partners were established after filtering. A total of 174 labeled proteins with high confidence were obtained (Fig. 2B). Among them, some proteins have been previously verified with or without functional phenotype, such as HSPA8 (7), cortactin (CTTN) (24), filamin A (FLNA) (24), LIM domain 7 (LMO7) (24), eukaryotic translation initiation factor 4 gamma 1 (EIF4G1) (25), heat shock protein 90β (26) (HSP90AB1, also known as HSP90B), and DEAD-box helicase 6 (DDX6) (27). Additionally, six proteins, including CTTN, LMO7, ACTR2, dynactin subunit 2 (DCTN2), spectrin alpha, non-erythrocytic 1 (SPTAN1), LIM, and calponin homology domains 1 (LIMCH1), were overlapped to a previous study (24) (Fig. 2C). Thus, the reliability of the results of the present study was confirmed.

These 174 proteins were analyzed by the Kyoto Encyclopedia of Genes and Genomes (KEGG), Gene Ontology (GO) and reactome analysis (Fig. 2D through F). The top 20 enriched proteins of KEGG revealed that the majority of these proteins were associated

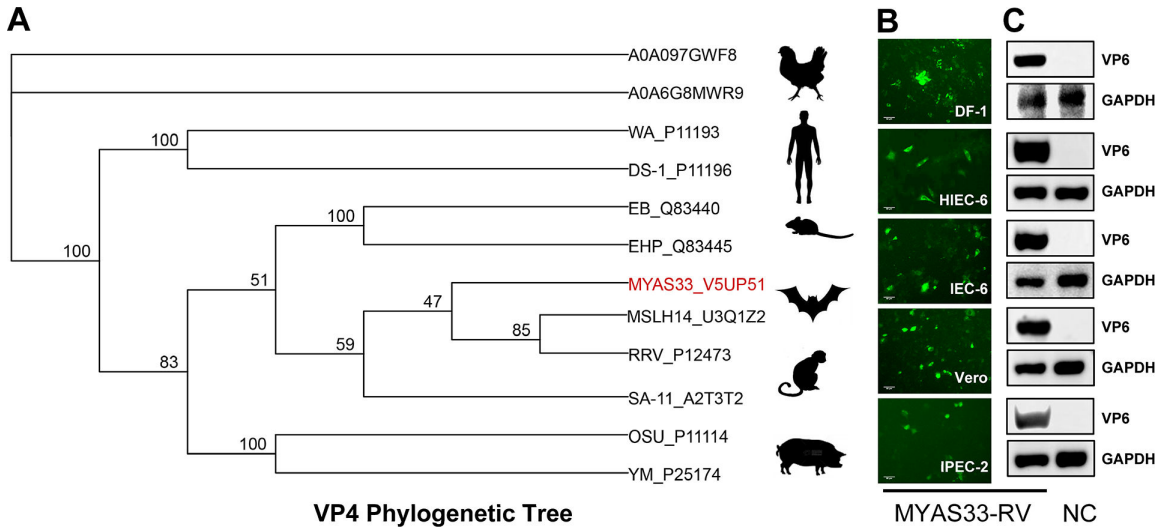

FIG 1 Characterization of RV strain applied in proximity labeling proteome. (A) Phylogenetic tree of RV based on VP4 proteins, which were representative of RV strains selected from human, chicken, mouse, bat, monkey, and pig. (B and C) Distinct cell lines that were challenged with MYAS33 were examined by immunofluorescence and Western blotting, and an anti-VP6 commercial antibody was used as a primary antibody.

with cytoskeleton function, including tight junction, endocytosis, and focal adhesion (Fig. 2D). And KEGG pathway analysis was also conducted (Fig. 2G).

Taken together, 174 high-confidence RV VP4-interacting proteins were detected and analyzed by the enrichment and KEGG pathway analysis.

VIM and ACTR2 promoted RV infection

The present study aimed to detect host proteins associated with RV entry, indicating that the candidate proteins were located in cytoskeleton, plasma membrane, and extracellular region. According to the GO cellular component classification (Fig. 3A), 88 proteins were located in the subcellular area (Fig. 3B). On the basis of the results of the GO analysis of these proteins, the top 20 enriched proteins were presented, and in biological level, the majority of proteins were associated with cytoskeleton organization, cellular localization, and organelle organization. On the molecular level, most of proteins were associated with cadherin binding, cell adhesion, molecular binding, and cytoskeletal protein binding (Fig. 3C).

To select appropriate research objects, an upset Venn graph was plotted to compare data sets of proteins according to location information, KEGG pathway enrichment analysis, omics data (unpublished), and published data (24) (Fig. 3D). The results showed that six proteins hit three points: HSPA8, HSP90AB1, FLNA, CTTN, VIM, and ACTR2. Importantly, four out of six proteins were verified as whether functional phenotypic proteins except for VIM and ACTR2 (7, 24, 26). Besides, BCAP31, which is a membrane protein, was also considered to be worthy of further investigation. Therefore, the three candidate genes were selected to further verify experimentally (Fig. 3E).

First, knockdown of VIM, ACTR2, and BCAP31 was conducted by small interfering RNA (siRNA) in MA104 and HIEC-6 cells, respectively (Fig. 4A). The best siRNAs were selected, which showed to have no significant effect on the cell viability (Fig. 4B). After knockdown of the three genes, challenged with MYAS33 strain for 24 h, *nsp5* gene-derived expression levels were measured through quantitative reverse transcription-polymerase chain reaction (RT-qPCR). As expected, the deletion of VIM and ACTR2 significantly decreased *nsp5* expression level compared with that induced by nonsense control RNA in both HIEC-6 and MA104 cells (Fig. 4C), suggesting that they may affect bat RV MYAS33 strain replication. However, BCAP31 reduced the above-mentioned effect only in MA104 cells, rather than in HIEC-6 cells.

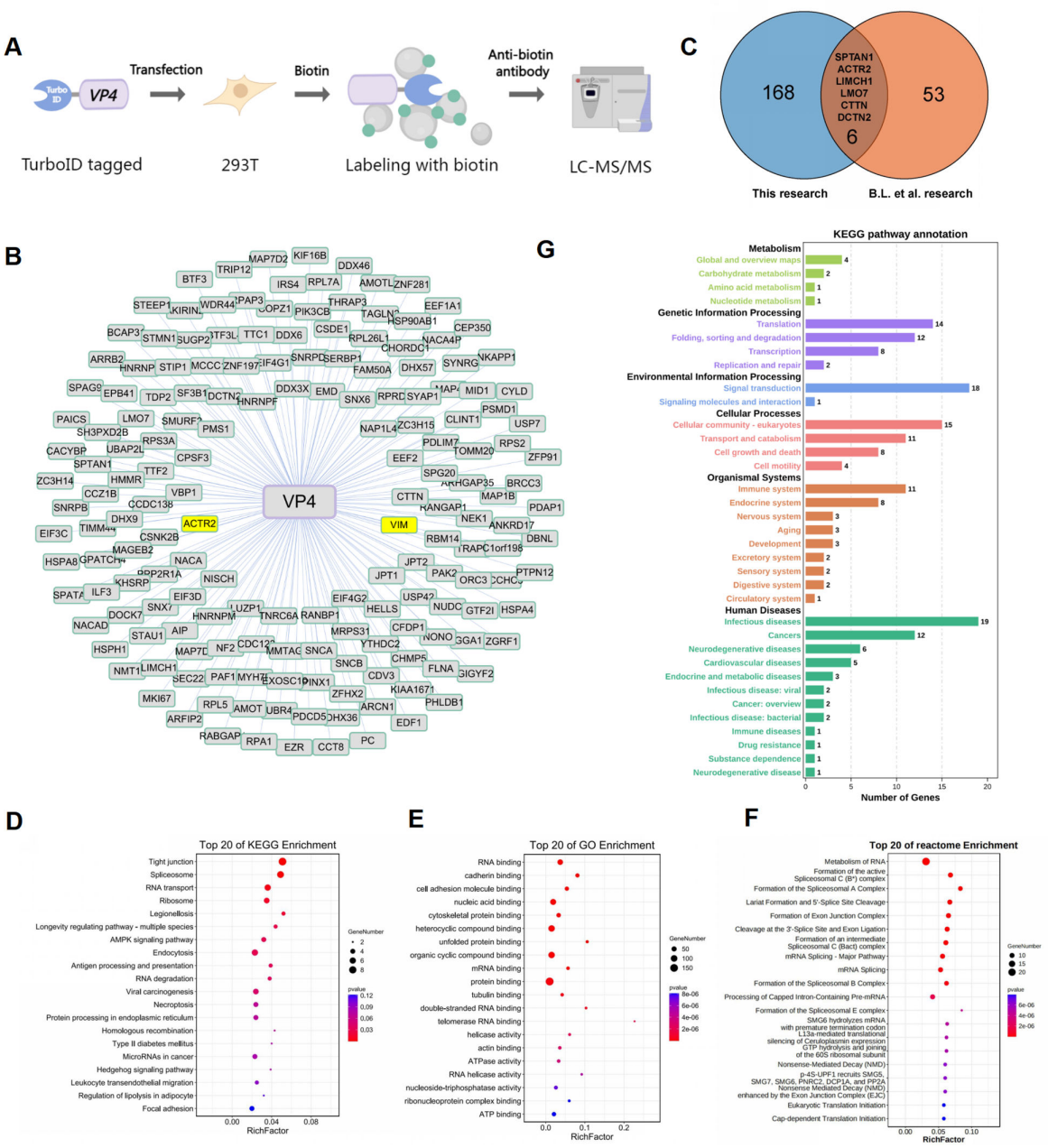

FIG 2 Global analysis of VP4 protein interactions. (A) Flowchart of the TurboID assay. (B) Interactions of VP4 and 174 high confidence proximity labeled host proteins. (C) The overlapped proteins of VP4 labeled proximity proteins and previous VP4 PPI data (24). (D through F) Top 20 terms of Kyoto Encyclopedia of Genes and Genomes (KEGG), Gene Ontology (GO), and reactome enrichment scheme. (G) KEGG pathway enrichment.

Taken together, it was concluded that the knockdown of VIM or ACTR2 significantly restricted RV infection in both MA104 and HIEC-6 cells. As human cells were targeted in the present study, VIM and ACTR2 were selected for further experiments.

VIM or ACTR2 interacted with VP4 and enhanced infection of different RV strains

According to the above-mentioned results, the physical interaction between VIM or ACTR2 and VP4 was examined, respectively. The results of co-immunoprecipitation (Co-IP) assay showed that both VIM and ACTR2 could interact with VP4 protein in HIEC-6 cells (Fig. 5A and B). Then, three additional species A RV strains, Wa human strain, SA11

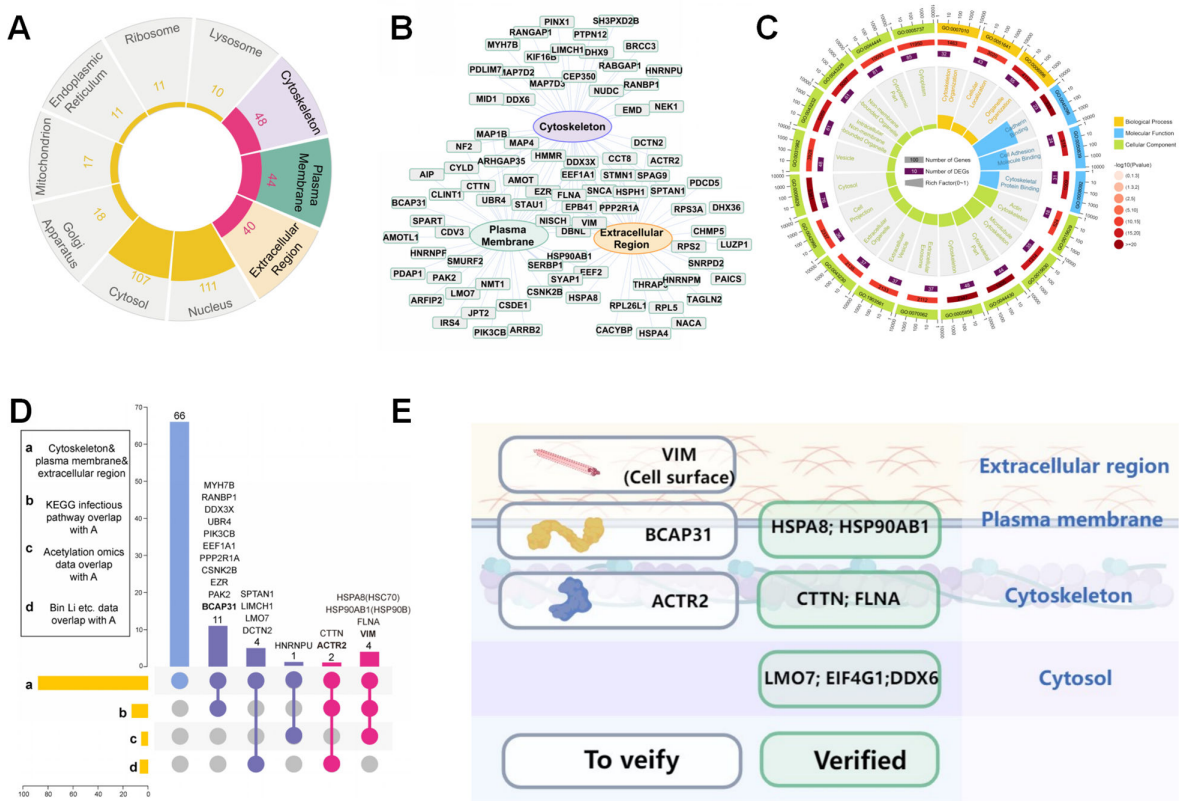

FIG 3 Analysis of proximity labeled proteins located in cytoskeleton, cell membrane, and extracellular region. (A) Subcellular distribution of VP4 proximity labeled proteins. (B) VP4 proximity labeled proteins located in cytoskeleton, plasma membrane, and extracellular region, (C) and top 20 terms of GO enrichment were presented. (D) Four data sets were used for making the comparison, which included VP4 proximity labeled proteins located in cytoskeleton, plasma membrane, and extracellular region, KEGG pathway infection-related protein, acetylation omics data, and Li et al. data. The comparison of the four data sets was presented as an upset Venn diagram, which suggested that VIM and ACTR2 hit three points. (E) VIM, BCAP31, and ACTR2 were selected to verify functional phenotype (white box), and proteins that have been verified function for RV infection were also presented (green box). HSPA8, HSP90, CTTN, DDX6 facilitate RV infection, and EIF4G1 inhibit RV infection, while FLNA and LMO7 have no obvious effect on RV infection.

monkey strain, and MSLH14 bat strain were used to further determine the activities of VIM and ACTR2. As expected, knockdown VIM or ACTR2 in HIEC-6 cells significantly reduced the infection of the three RV strains at mRNA level (Fig. 5C through E).

These results further demonstrated that both VIM and ACTR2 potentially enhanced infection of different RV strains. As human RV was targeted in the present study, the human RV Wa strain was selected for further in-depth research.

Loss of function of VIM or ACTR2 restricted infection of the human RV Wa strain in HIEC-6 cells

To further examine whether VIM or ACTR2 could decrease RV protein expression or RV replication, siRNA knockdown and antibody-blocking experiments were performed. The VIM activity was determined by detecting VP6 protein expression using immunofluorescence, Western blotting, and flow cytometry. As shown in Fig. 6A and B, compared with si-NC negative control (NC) cells, knockdown of VIM significantly decreased fluorescence, and the VP6 protein expression was significantly reduced at 12 and 24 h. Then, flow cytometry was carried out using fluorescein isothiocyanate (FITC)-conjugated anti-RV antibody to measure the proportion of RV-positive cells. After being challenged with RV for 24 h, the proportion of FITC-positive cells in NC group was 8.91% ± 1.70%, while it was 1.35% ± 0.22% in VIM knockdown HIEC-6 cells (Fig. 6C). Moreover, the RV titer in VIM knockdown HIEC-6 cells was subsequently determined at 12 and 24 h. Compared with NC cells, the titer was about 10× lower in VIM-KD cells at 12 h (Fig. 6D). Considering the

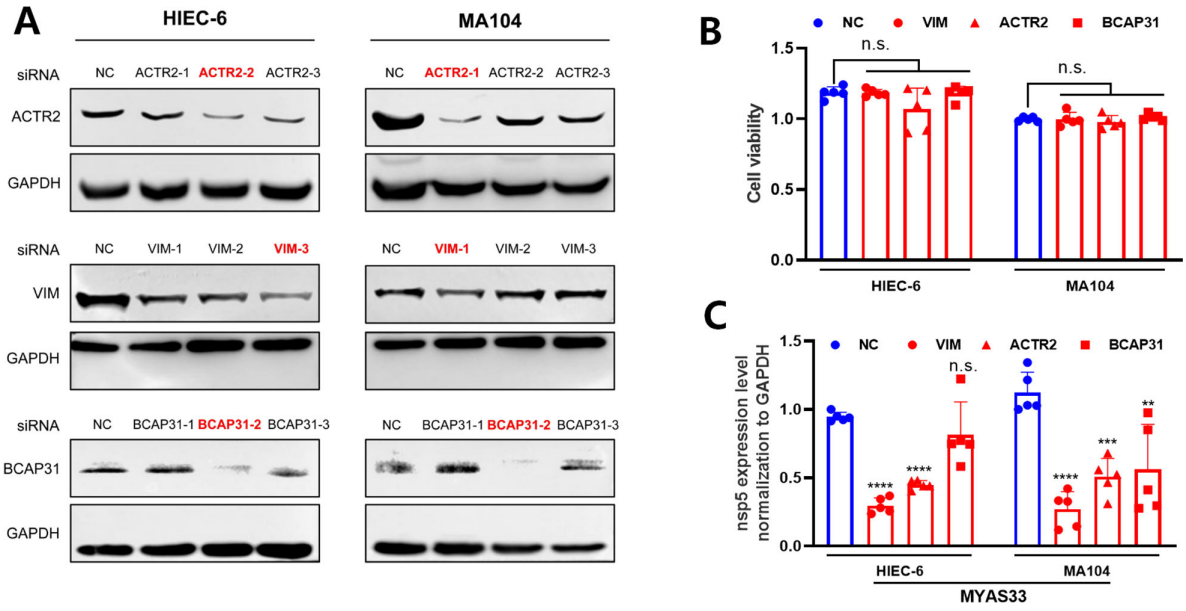

FIG 4 VIM and ACTR2 promoted MYAS33 RV strain infection in both HIEC-6 and MA104 cells.(A) Three siRNAs of each target gene were applied to HIEC-6 and MA104 cells, some siRNAs can partially knock down the target protein, and those with the best knockdown effect (red) were applied to the experiments. (B) Cells that transfected siRNAs were measured for cell viability by CCK8 at 24 h. (C) Knockdown of VIM and ACTR2 restricted MYAS33 (0.1 MOI) proliferation in both HIEC-6 and MA104 cells, and knockdown of BCAP31 restricted MYAS33 (0.1 MOI) proliferation in MA104 cells, rather than in HIEC-6 cells, as examined by RT-qPCR (24 h). Statistical significance was determined by the Student's *t*-test (*<0.05; **$P < 0.01$; ***$P < 0.001$; ****$P < 0.0001$; n.s., not significant).

potential function and location of VIM, we speculated that VIM might affect RV infection at an early step, and we detected the earlier time points of RV infection (1, 2, 4, and 6 h), which suggested that VIM effect RV infection at the early stage (Fig. 6E). VIM polyclonal antibody was applied to block HIEC-6 cell surface VIM, and immunoglobulin G (IgG) was added as NC. The cells were then infected at a multiplicity of infection (MOI) of 0.1, and RV proliferation was examined by RT-qPCR and titer. The results suggested that the VIM antibody decreased RV proliferation at 24 h (Fig. 6F and G). Collectively, loss of VIM function restricted the human RV Wa strain infection in HIEC-6 cells.

A series of experiments consistent with the study of VIM were conducted to verify the effects of ACTR2 on RV infection. The results of immunofluorescence (Fig. 7A), Western blotting (Fig. 7B), flow cytometry (Fig. 7C), and viral titer examination (Fig. 7D) suggested that knockdown of ACTR2 inhibited RV infection. Besides, ACTR2 also affects RV infection at an early stage (Fig. 7E), and blocking HIEC-6 by antibody also restricted RV infection, as evidenced by RT-qPCR (Fig. 7F) and viral titer (Fig. 7G).

Taken together, both VIM and ACTR2 significantly promoted RV infection in human intestinal cells via knockdown or antibody blockage.

Overexpression or pretreatment with recombinant protein of VIM or ACTR2 promoted the human RV Wa strain infection in CACO-2 cells

CACO-2 cells were transfected with VIM or ACTR2 expression plasmid for 24 h and were then infected with RV. Furthermore, *nsp5* relative expression level (Fig. 8A and B) and viral titer (Fig. 8C and D) were examined at 24 h, and the results suggested that overexpression of VIM or ACTR2 promoted RV infection.

In order to increase the cell surface VIM or ACTR2, recombinant human VIM or ACTR2 (Fig. 8E and F) was added to CACO-2 cells with concentrations of 0.5 or 1.0 µg, and bovine serum albumin (BSA) was added as NC. The cells were then challenged with 0.1 MOI RV, and *nsp5* relative expression level (Fig. 8G and H) and viral titer (Fig. 8I and J) were determined at 24 h post-infection. The results showed that recombinant human

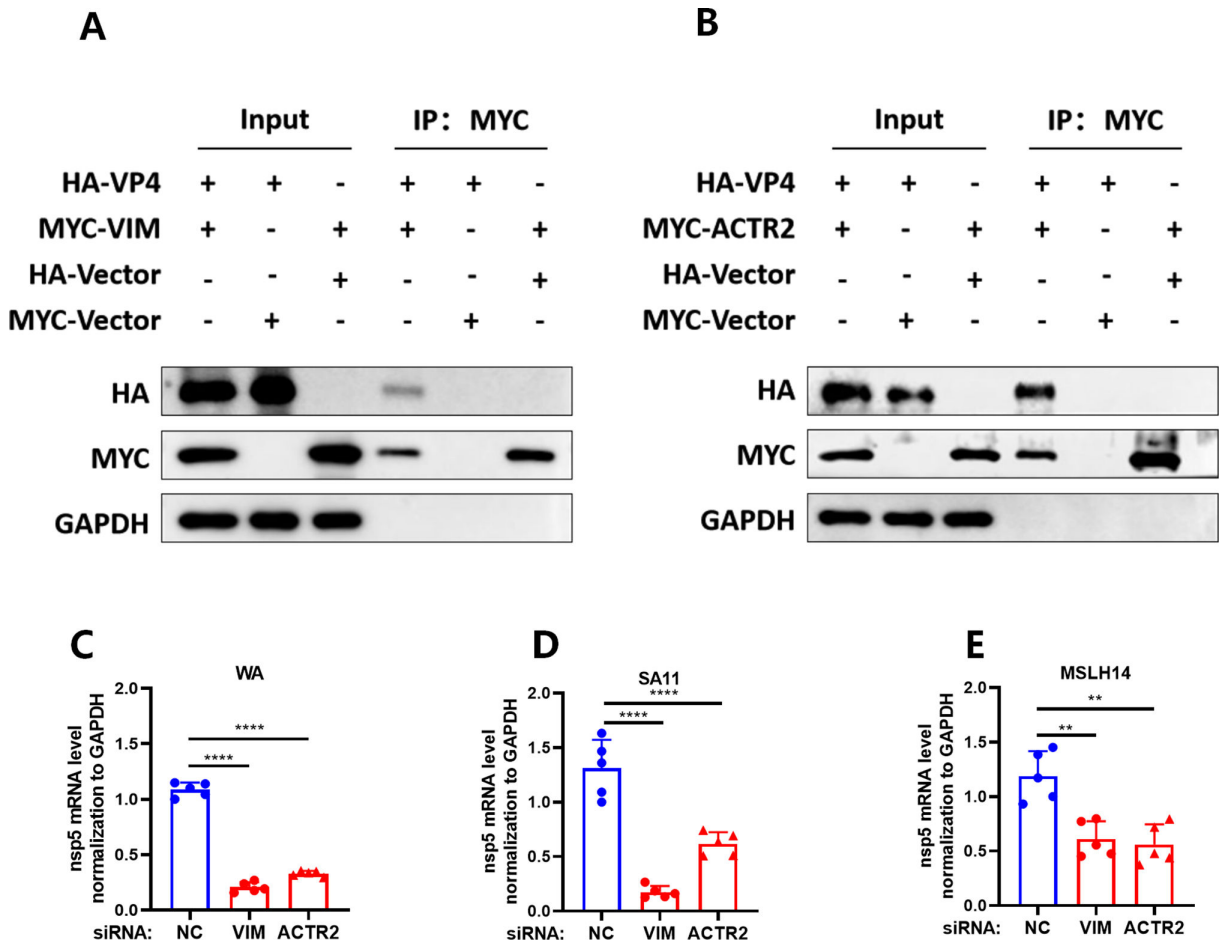

FIG 5 Knockdown of VIM or ACTR2 also restricted the other three RV strains, and VP4 interacted with VIM or ACTR2. (A and B) Myc-VIM (or Myc-ACTR2) and HA-VP4 plasmids were transfected to HEK293T cells, and anti-Myc IPs were analyzed by immunoblotting with HA and Myc antibodies. (C–E) Knockdown of VIM or ACTR2 in HIEC-6 cells also restricted the replication of three other RV strains in mRNA level. Statistical significance was determined by the Student's *t*-test (*<0.05; **$P < 0.01$; ***$P < 0.001$; ****$P < 0.0001$; n.s., not significant).

VIM or ACTR2 promoted RV infection. Collectively, overexpression or pretreatment with recombinant protein of VIM or ACTR2 promoted RV infection in CACO-2 cells.

VIM and ACTR2 increased the efficiency of binding of the human RV Wa strain to HIEC-6 cells

Several assays were conducted to explore whether VIM or ACTR2 could increase the efficiency of RV binding. VIM or ACTR2 present on the HIEC-6 surface was observed by a confocal microscope (z-stack imaging), and the results suggested that some VIM or ACTR2 can be observed on the HIEC-6 surface (Fig. 9A). Flow cytometry further confirmed the existence of VIM or ACTR2 on the HIEC-6 surface (Fig. 9B and C). Binding assays were then conducted to verify whether VIM or ACTR2 could participate in RV attachment (24, 28) (Fig. 9D). Moreover, knockdown HIEC-6 cells were challenged with RV at an MOI of 10 for 1 h at 4°C, and *nsp5* relative expression level and *VP6* absolute expression level were measured by RT-qPCR, which showed a decrease in VIM or ACTR2 knockdown cells compared with NC cells (Fig. 9E and F K, and L). The polyclonal antibody was then added to HIEC-6 cells and incubated at 37°C for 1 h, followed by challenging with 10 MOI RV for 1 h at 4°C, which showed a reduction of RV infection after incubation with VIM or ACTR2 antibody compared with NC group (Fig. 9G and H). Subsequently, the same procedure was conducted for RV challenge or pretreatment with recombinant protein of VIM or ACTR2, and the results indicated that recombinant VIM or ACTR2

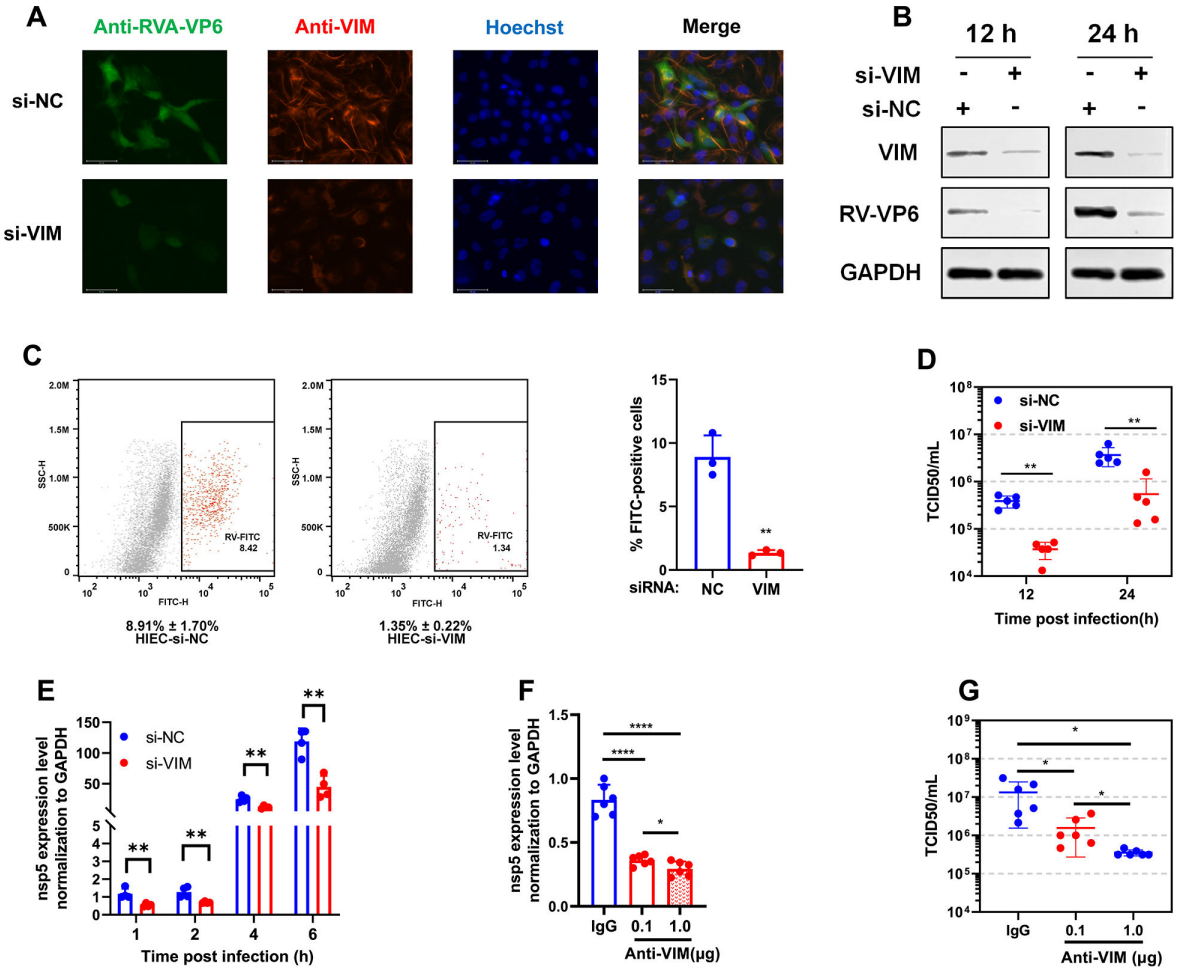

FIG 6 Knockdown of VIM or blocking cell surface of VIM restricted Wa RV strain infection in HIEC-6 cells. Knockdown of VIM in HIEC-6 cells restricted RV infection, as examined by (A) immunofluorescence (24 h) and (B) Western blotting (12 and 24 h) with anti-VP6 antibody as a primary antibody, and (C) flow cytometry with FITC-conjugated anti-RV antibody. (D) Viral titer was detected at 12 h and 24 h p.i.. (E) More earlier time points of RV infection were further detected by RT-qPCR, which suggested VIM affects RV infection at an early stage. HIEC-6 cells were plated into 96 wells and pretreated with VIM antibody, challenged with 0.1 MOI RV, and (F) RT-qPCR and (G) viral titer examinations were then performed.

increased the efficiency of RV binding (Fig. 9I and J M, and N). Taken together, VIM and ACTR2 could be found on HICE-6 cell surface and significantly increased the efficiency of binding of the human RV Wa strain to HICE-6 cells.

VIM and ACTR2 exhibited to have synergistic effects on promoting RV infection

Due to the similar functions of VIM and ACTR2, it was attempted to indicate whether they have synergistic effects. Then, VIM and ACTR2 were simultaneously or separately knocked down to identify the relationship. The results revealed that the simultaneous knockdown of VIM and ACTR2 had a more significant restrictive effect than separate knockdown (Fig. 10), suggesting that VIM and ACTR2 synergistically promoted RV infection.

DISCUSSION

RV is one of the most important pathogens for humans and animals with diarrhea. Although several studies have concentrated on RV entry, further research should be conducted to eliminate some gaps. To date, numerous proteins or carbohydrates have been reported to participate in RV entry, such as HGBAs, SA, HSPA8, integrins, etc. (3).

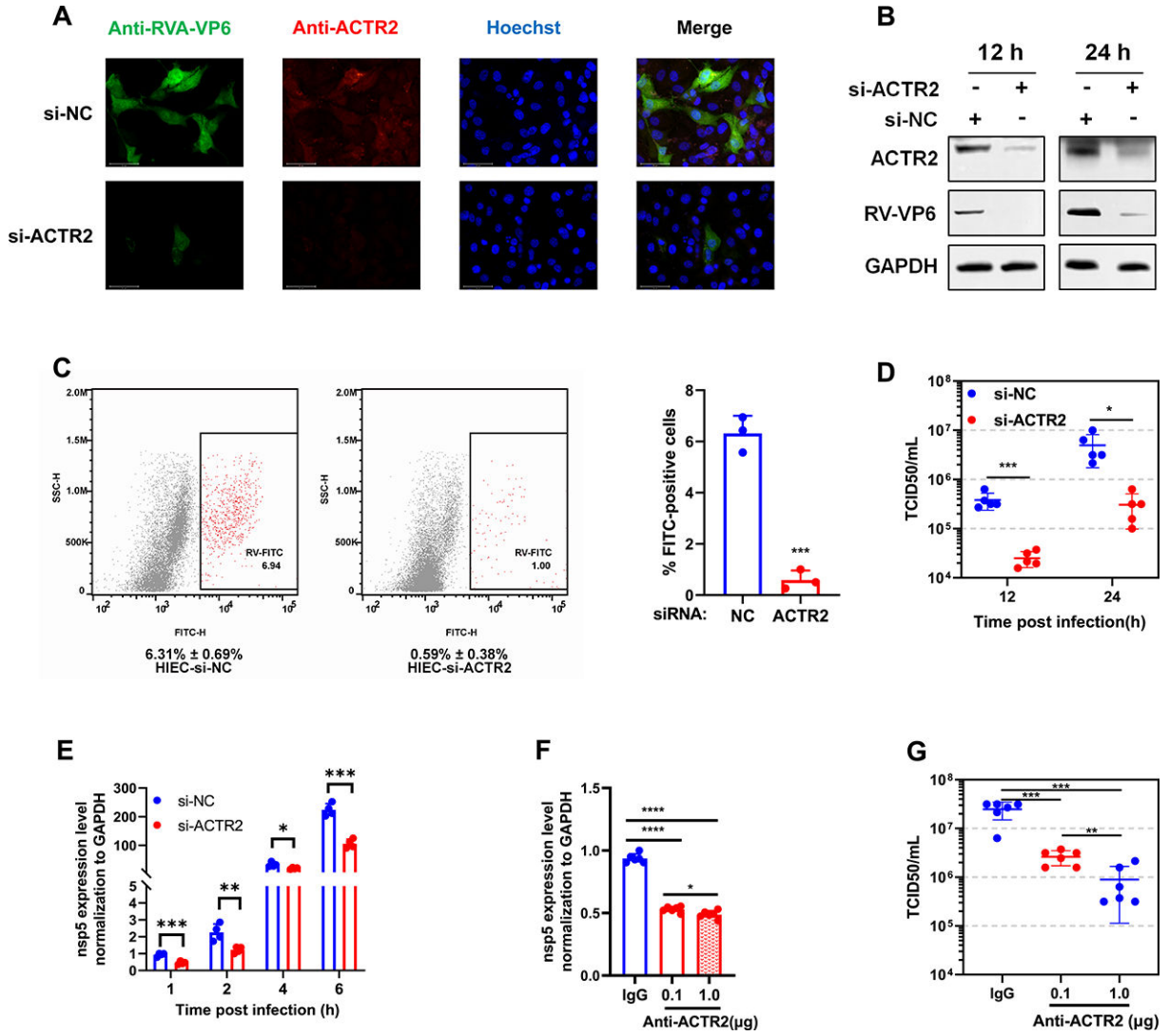

FIG 7 Knockdown of ACTR2 or blocking cell surface of ACTR2 restricted Wa RV strain infection in HIEC-6 cells. Knockdown of ACTR2 in HIEC-6 cells restricted RV infection, as examined by (A) immunofluorescence (24 h) and (B) Western blotting (12 and 24 h) with anti-VP6 antibody as a primary antibody, and (C) flow cytometry with FITC-conjugated anti-RV antibody. (D) Viral titer was detected at 12 and 24 h. (E) More earlier time points of RV infection were further detected by RT-qPCR, which suggested ACTR2 affects RV infection at an early stage. HIEC-6 cells were plated into 96 wells and pretreated with ACTR2 antibody, challenged with 0.1 MOI RV, and (F) RT-qPCR, and (G) viral titer examinations were then performed.

It is noteworthy that VP4 was considered as the most significant viral protein. Although there has been an excellent systematic research to detect VP4 and host-pathogen PPI network (24), not many generally accepted attachment factor of RV has yet been reported; thus, a proximity interactome labeling technique was applied to detect VP4 and host-pathogen PPI network in the present study. The VP4 was amplified from a type A RV, and it was verified that this strain had a broad-spectrum cellular infection. Additionally, HIEC-6 and DF-1 cells were first applied to RV infection research, providing new cell lines for research of RV *in vitro*. From our perspective, HIEC-6 is a normal human intestinal cell line, which may possess advantages over the carcinoma cell line, and DF-1 is an avian cell line, which may benefit to avian RV research. As for the research method, the proximity labeling approach was employed to detect VP4 protein and host-pathogen PPI network. In total, 174 high-confidence proximity-labeled host proteins were detected, and a series of analyses were conducted. Among the host proteins, HSPA8, CTTN, HSP90AB1, and EIF4G1 have been reported to participate in RV infection, and

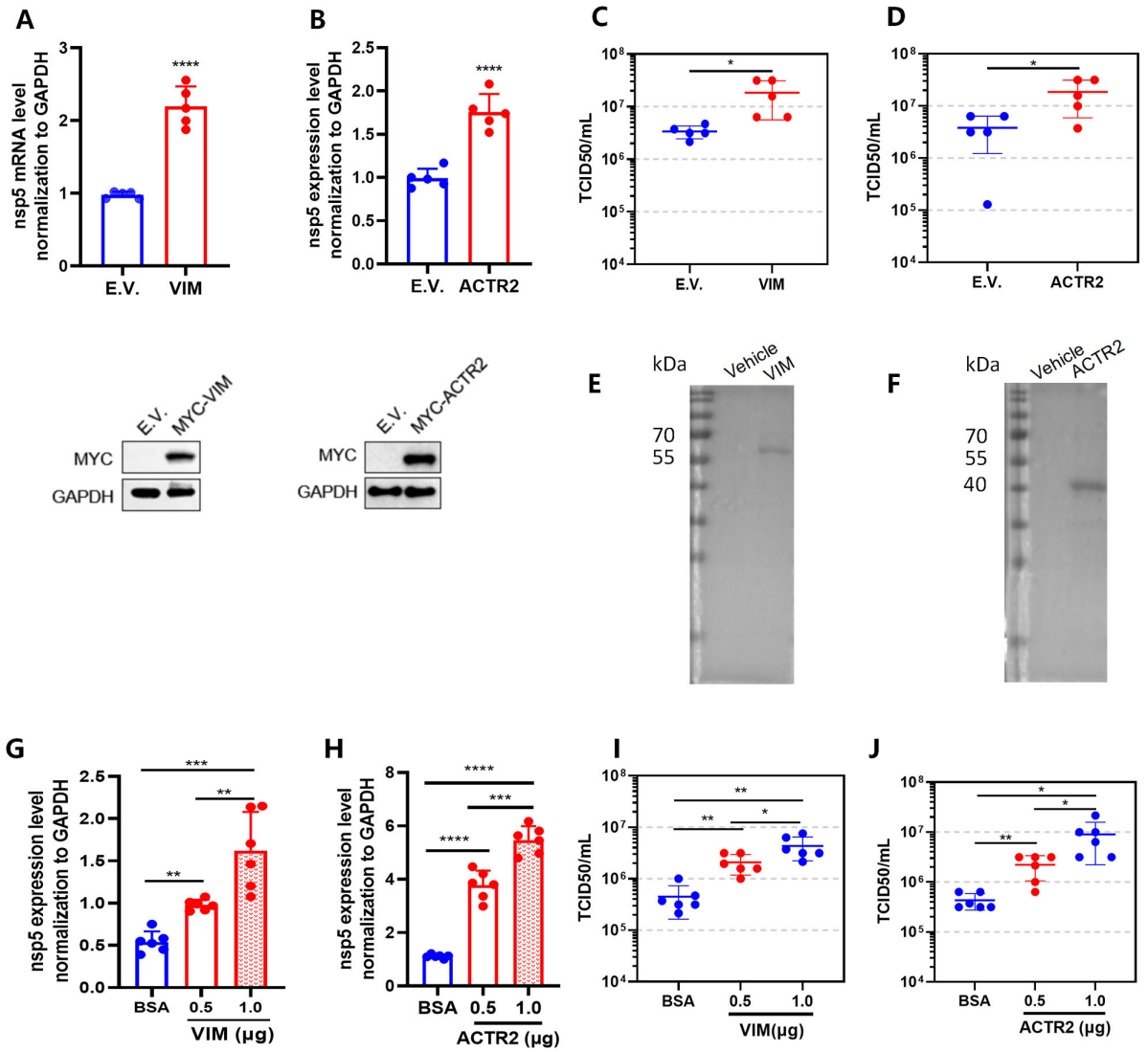

FIG 8 Overexpression or pretreatment with recombinant of VIM or ACTR2 promoted Wa RV strain infection in CACO-2 cells. VIM or ACTR2 was overexpressed in CACO-2 cells, challenged with 0.1 MOI RV at 24 h post-transfection, and examined (A and B) RT-qPCR and (C and D) viral titer examinations at 24 h post-infection, the expression control of VIM and ACTR2 were presented below. (E and F) The purification of VIM and ACTR2 was identified by sodium dodecyl sulfate-polyacrylamide gel electrophoresis (SDS-PAGE) staining with Coomassie brilliant blue. VIM or ACTR2 recombinant protein was incubated, challenged with 0.1 MOI RV, and (G and H) RT-qPCR and (I and J) viral titer examinations were carried out. E.V.: empty vector. Statistical significance was determined by the Student's *t*-test (*<0.05; **P < 0.01; ***P < 0.001; ****P < 0.0001; n.s., not significant).

FLNA and LMO7 exhibited to have no significant phenotypic effect on RV infection (24), these reported proteins proved the reliability of our atlas to some extent.

The subcellular location of candidate receptors or attachment factors is crucial, which are supposed to be distributed in cytoskeleton, plasma membrane, or extracellular region. Additionally, proteins that were detected in both Li et al. research (24) and, in the present study, may be considered to be more reliable. Besides, we also consulted infectious disease pathway and our unpublished acetylation omics. The sample of this acetylation omics was HIEC-6 cell line that was challenged with MYAS33, and acetylation affected multiple biological functions, containing the PPI network. Finally, six proteins (HSPA8, VIM, CTTN, HSP90AB1, FLNA, and ACTR2) were selected. Importantly, except for VIM and ACTR2, the other four proteins have verified whether had the function in RV infection.

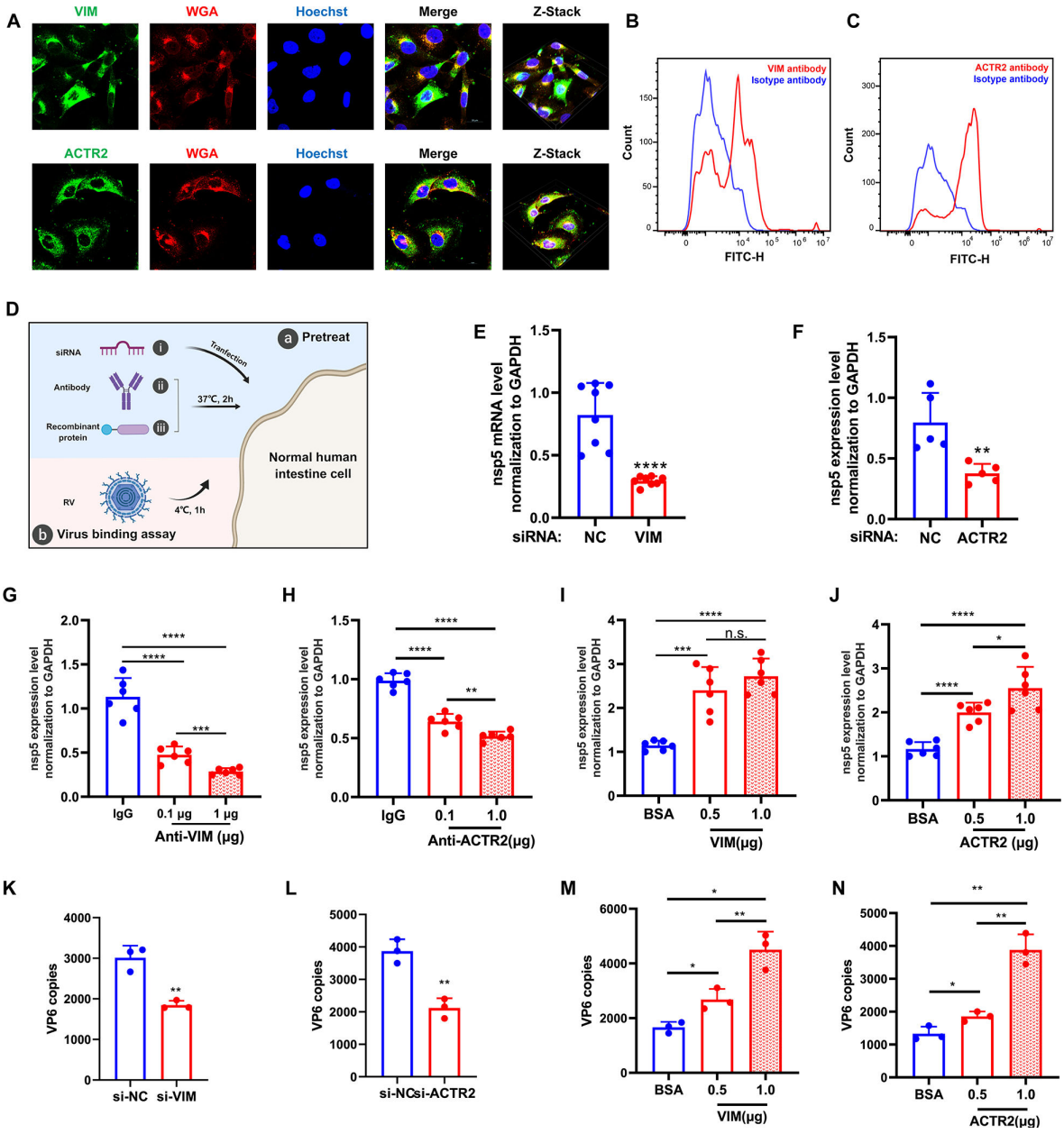

FIG 9 VIM and ACTR2 increased the efficiency of binding of Wa RV strain to HIEC-6 cells. (A) HIEC-6 cells were stained with VIM or ACTR2 antibodies, WGA and hoechst. They were captured by a confocal microscope (z-stack imaging) and showed VIM or ACTR2 (green), WGA (red), and hoechst (blue). (B and C) HIEC-6 cells were stained with VIM antibody or ACTR2 antibody (red) or rabbit IgG as isotype antibody (blue) as a primary antibody and anti-rabbit FITC antibody as a secondary antibody, and the results were examined by flow cytometry. (D) The schematic model of RV binding assays. (E and F) VIM or ACTR2 siRNAs were transfected to HIEC-6 cells for 24 h and incubated with 10 MOI RV at 4°C, and the nsp5 relative level were examined by RT-qPCR. HIEC-6 cells were then plated into 96 wells, pretreated with VIM or ACTR2 antibody or recombinant protein for 2 h at 37°C, and incubated with 10 MOI RV for 1 h at 4°C, and the (G through J) nsp5 relative level and (K through N) VP6 absolute quantification were examined by RT-qPCR. Statistical significance is determined by the Student's *t*-test (*<0.05; **$P < 0.01$; ***$P < 0.001$; ****$P < 0.0001$; n.s., not significant).

VIM is one of the intermediate filament proteins, which is widely expressed in multiple cell lines and is located in the extracellular region, cytoskeleton (29). VIM has been demonstrated to promote viral entry as an attachment factor for SARS-CoV-2 (30, 31), SARS-CoV (32), enterovirus 71 (33), Japanese encephalitis virus (JEV) (34, 35), and human papillomavirus 16 (HPV16) (36). As for RV, Brunet JP et al. found that the VIM network disorganization detected in undifferentiated CACO-2 cells was not found in fully

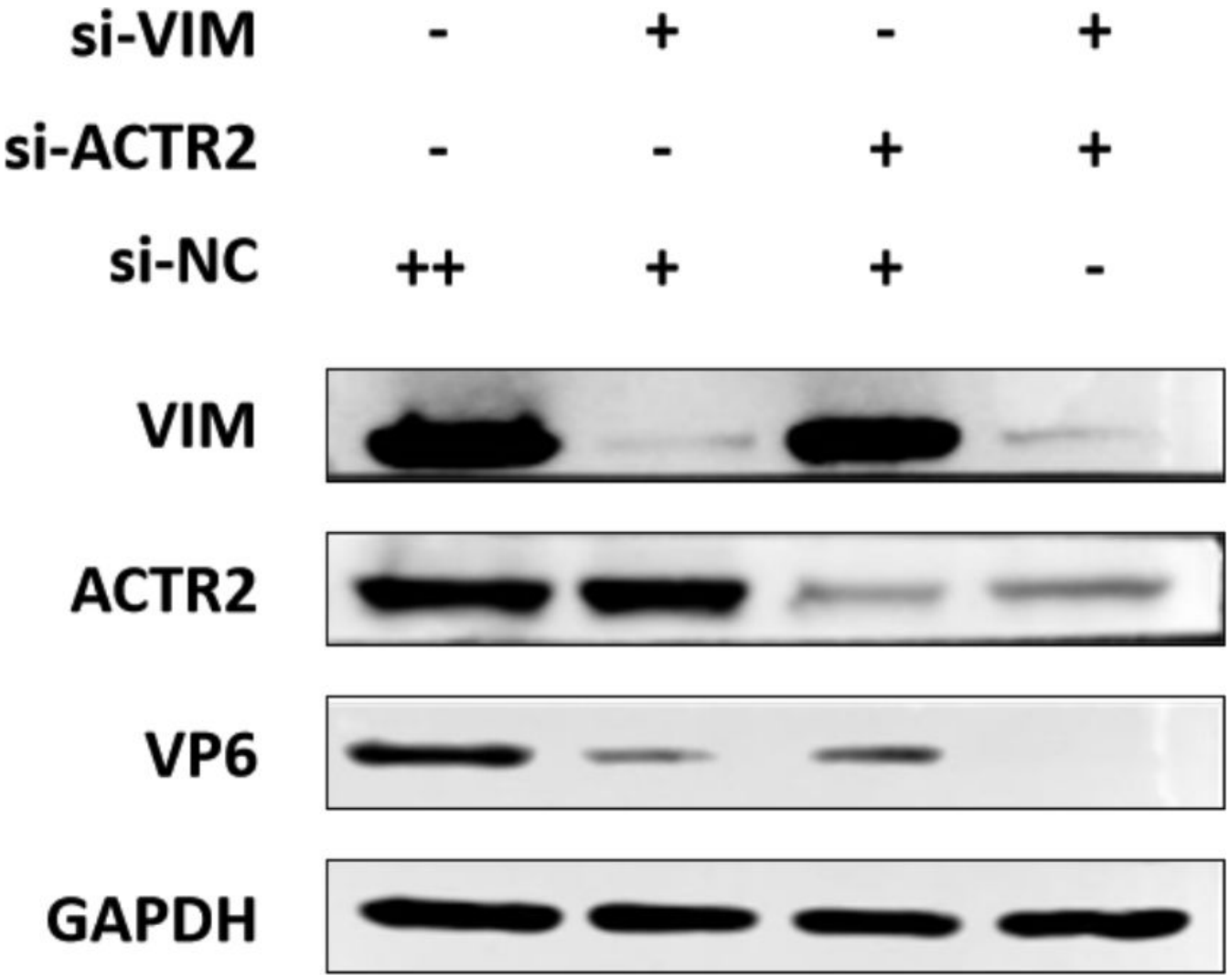

FIG. 10 VIM and ACTR2 promoted RV infection. VIM and ACTR2 were knocked down simultaneously or separately in HIEC-6 cells and challenged with 0.1 MOI RV for 24 h, and the results were examined by Western blotting.

differentiated cells (37), and in the present study, VIM was selected to further determine whether VIM would be an attachment factor for RV.

ACTR2 is recognized as a major constituent of the ARP2/3 complex, which is mainly located at the skeleton, and it is essential to cell shape and motility (38). It has been reported that ACTR2 participates in various viral infections, such as respiratory syncytial virus (39, 40), Ebola virus (41), vaccinia virus (42), and JEV (43).

In the present study, it was confirmed that both VIM and ACTR2 could facilitate RV infection in human intestinal cells. According to previous research or GO enrichment, both VIM and ACTR2 could be located in the extracellular region, so we wonder whether VIM and ACTR2 could promote RV attachment. Additionally, it was revealed that they could promote RV binding through knockdown, antibody blockade, and recombinant protein incubation. Of course, these proteins may promote RV infection through other ways, such as whether ARP2/3 complex plays an important role in RV infection, whether VIM can promote RV infection by inhibiting interferon production (44), and we will explore the further mechanisms in the future.

In conclusion, we provide an atlas of RV VP4 PPI network, and it was demonstrated that both VIM and ACTR2 could significantly promote RV infection.

MATERIALS AND METHODS

Cells and viruses

HIEC-6 and MA104 cells were purchased from BeNa Culture Collection, and HEK293T, DF-1, CACO-2 cells were preserved in our laboratory. All cells were cultured in a Dulbecco's modified Eagle's medium (DMEM; Gibco, New York, NY, USA) containing 10% fetal bovine serum (Gibco) and 1% penicillin-streptomycin solution (Hyclone Laboratories, Logan, UT, USA).

The RV strain MYAS33 and MSLH14 were originally isolated by C.C.Tu's laboratory as described previously (23, 45). The human RV Wa and SA-11 RV strain were kindly provided by Prof. Wu Yuzhang, Institute of Immunology, PLA, Army Medical University, and propagation and titration of MA104 cells were carried out as previously described (46, 47). For RV infection, the virus was diluted in DMEM, activated with 10 µg/mL trypsin (Solarbio, Beijing, China; T1350) for 30 min at 37°C, and was then added to confluent target cells that were previously thrice washed with phosphate-buffered saline (PBS). After 2 h of incubation at 37°C, the excessive virus was removed; the cells were then twice washed with PBS and incubated in a DMEM with 2 µg/mL trypsin at 37°C until use.

Proximity labeling with TurboID assays, MS analysis, data processing, and bioinformatics analysis

VP4 protein coding sequence was amplified from MYAS33 and cloned into pcDNA3.1-TurboID vector. The plasmid was transfected into HEK293T cells and added to biotin (50 µm) for 10 min. The protocols of proximity labeling with TurboID assays, MS analysis, data processing, and bioinformatics analysis were the same as those that were previously described (13, 48, 49).

Antibodies and reagents

Antibodies against VIM (cat# 10366–1-AP), ACTR2 (cat# 10922–1-AP), and BCAP31 (cat# 11200–1-AP) were purchased from Proteintech (San Diego, CA, USA). Antibody against RV VP6 protein (cat# sc-101363) was purchased from Santa Cruz Biotechnology (Dallas, TX, USA). Anti-RV antibody (FITC; cat# ab31435) was purchased from Abcam (Cambridge, UK). Antibodies against GAPDH (cat# 5174) and Myc (cat# 2276) were purchased from Cell Signaling Technology (Danvers, MA, USA). HA Tag rabbit polyclonal antibody (cat# AF0039), horseradish peroxidase (HRP)-labeled goat anti-rabbit IgG(H + L; cat# A0208), HRP-labeled goat anti-mouse IgG (H + L; cat# A0216), Cy3-labeled goat anti-rabbit IgG (H + L; cat# A0516), and FITC-labeled goat anti-mouse IgG (H + L; cat# A0568) antibodies were purchased from Beyotime Institute of Biotechnology (Shanghai, China).

Lipofectamine RNAiMAX (cat# 13778030) and Lipofectamine 3,000 (cat# L3000150) were purchased from Invitrogen (Carlsbad, CA, USA). Recombinant human VIM protein (cat# 10028-H08B) was obtained from Sinobiological Co., Ltd. (Shenzhen, China). Recombinant ACTR2 protein (cat#P03403) and iFluor 555 WGA (Cat#I3310) were purchased from Solarbio Co., Ltd. Rabbit IgG (cat#A7016), BSA (cat# ST023), and cell counting kit-8 (cat# C0037) were purchased from Beyotime Institute of Biotechnology.

Plasmids, siRNA, and transfection

Human VIM and ACTR2 coding sequences were amplified from HIEC-6, which were identical to NCBI reference sequences of NM_003380.5 and NM_005722.4, respectively, and were then cloned to pcDNA3.1–3Myc vector, which was digested by BamHI and NotI previously. RV VP4 protein was cloned to pcDNA3.1–3HA vector for immunoprecipitation. All the ligation products were transformed into Trans-T1 competent cells and plated on ampicillin-resistant agar plates, single clones were picked and shaken in a 37°C incubator, and plasmids were extracted and identified.

The cells were grown to 80% confluence prior to transfection, and plasmids were transfected with Lipofectamine 3,000 for 24 h according to the manufacturer's instructions.

Moreover, siRNAs of VIM (cat# SIGS0005747-1), ACTR2 (cat# SIGS0004877-1), and BCAP31 (cat# SIGS0003096-1) were purchased from RiboBio Co., Ltd. (Guangzhou, China). The cells were grown to 80%–90% confluence prior to transfection, transfected with siRNAs using Lipofectamine RNAiMAX for 48 h, and were then detected or used for further experiment.

Virus-binding assay

HIEC-6 cells were seeded into 24-well or 96-well plates and grown to 80%–90% confluence. In 24-well plates, HIEC-6 cells were transfected with VIM or ACTR2 siRNA for 48 h, and in 96-well plates, HIEC-6 cells were incubated with VIM or ACTR2 recombinant protein or antibody for 2 h at 37°C. After pretreatment, the cells were twice washed with pre-cooled PBS and incubated with RV (10 MOI) at 4°C for 1 h. The cells were then twice washed with PBS and detected by RT-qPCR.

Western blotting

The main method of western blotting was described previously (49). Cells were collected and lysed, and protein concentrations were determined by a bicinchoninic acid (BCA) protein assay kit (P0010; Beyotime Institute of Biotechnology). The proteins were mixed with loading buffer and denatured by boiling. Then, equal amounts (30 µg) were electrophoresed, transferred onto nitrocellulose filter membranes, and were then incubated overnight at 4°C with primary antibodies. After further incubation with HRP-conjugated secondary antibodies, the membranes were detected by the Amersham Imaging 600 system, with Pierce ECL Western blotting substrate (32106; Thermo Fisher Scientific).

Immunoprecipitation

In the present study, 2 µg of 3HA-VP4, 3Myc-VIM (or ACTR2), or vector were transfected into 2×10^6 HEK293T cells in 6-well plates, harvested after 30 h, and lysed by 200 µL lysis buffer (P0013; Beyotime Institute of Biotechnology). Twenty percent of the cell lysates were separated as an input, and the remaining lysates were incubated with 20 µL of anti-Myc (Bimake; B26301) magnetic beads on a roller at 4°C overnight. The beads were washed five times with 1 mL lysis buffer and boiled at 100°C for 10 min. Cell lysates and IPs were analyzed by Western blotting.

RNA isolation and quantitative real-time PCR analysis

Cells were collected, and total RNA was isolated by an RNA extractor (TRIzol; B511311; Sangon Biotech Co., Ltd., Shanghai, China) and were then reversely transcribed by a premix reverse transcriptase (R222-01; Vazyme Co., Ltd., Nanjing, China), 1 µg RNA and 4 µL 5× Hiscript II qRT SurperMix were mixed and added H_2O to 20 µl, and put the mixture in a 50°C water bath for 15 min and 85°C for 5 s.

The qPCR was then conducted by an SYBR Green qPCR Mix kit (A6001; Promega, Beijing, China) and a CFX96 system. All experiments were performed according to the manufacturer's instructions. The specific primers used to RT-qPCR were as follows: for the GAPDH, 123 bp (amplicon), 5′-CTACATGGTTTACATGTTCC-3′ (Forward) and 5′-GGATCTCG CTCCTGGAAGAT-3′ (Reverse); for the nsp5, 178 bp (amplicon), 5′-CGTCAACTCTTTCTGG AAAATC-3′ (Forward) and 5′-GCATTTGTCTTAACTGCATTCG-3′ (Reverse); for VP6, 147 bp (amplicon), 5′-CATGCGCCATAAATGCACCA-3′ (Forward) and 5′-TCGCGCCATCAGCTGAATTA -3′ (Reverse).

Immunofluorescence and confocal assay

Cells were fixed with 4% paraformaldehyde solution (P1110; Solarbio) for 1 h. Washed thrice, and the cells were blocked by BSA for 1 h. After washing thrice, specific primary antibodies were added and incubated overnight at 4°C. Cells were then washed and incubated with the anti-rabbit or anti-mouse fluorescent secondary antibodies for 1 h. Images were captured by a fluorescence or a confocal microscope.

Flow cytometry

Cells were digested by trypsin and collected. After twice washing with PBS, the cells fixed by 4% paraformaldehyde, were incubated with the FITC-conjugated RV antibody for 30 min at 4°C (for RV staining, permeabilized before staining), or incubated with primary antibody for 30 min at 4°C, washed thrice with PBS, then incubated with secondary antibody for 30 min at 4°C (for cell surface staining, not permeabilized, the same isotype control was applied and compared to VIM and ACTR2 respectively.). After washing thrice with PBS, the cells were re-suspended in 200 µL PBS solution per sample. Fluorescence intensity was determined and analyzed using the CytoFlEX system (Beckman Coulter, Brea, CA, USA).

Statistical analysis

Statistical significance between groups was determined using GraphPad Prism 8.0 software (GraphPad Software Inc., San Diego, CA, USA). Data were presented as mean ± SEM in all experiments and analyzed using *t*-test or analysis of variance, followed by two-tailed *t*-test. $P < 0.05$ was considered statistically significant.

ACKNOWLEDGMENTS

This study was financially supported by the National Key Research and Development Program of China (Grant No. 2021YFD1801103-6), the National Natural Science Foundation of China (Grant No. 31972719), and the CAMS Innovation Fund for Medical Sciences (Grant No. 2020-12M-5-001).

Conceptualization, N.J., C.L., J.W. and P.H. Data curation, C.L., J.W. and P.H. Software, L.S. and C.J. Supervision, N.J., C.L. and J.W. Funding acquisition, N.J., C.L., and L.L. Validation, N.J., C.L., J.W. and P.H. Investigation, P.H., Q.Q., L.L., W.X., S.D., Z.H., Y.J., J.C., and Z.G. Methodology, P.H., Q.Q., L.L., W.X., S.D., Z.H., Y.J., J.C., and Z.G. Writing-original draft, P.H. Project administration, N.J., C.L., and L.L. Writing-review and editing, N.J., C.L., J.W.

AUTHOR AFFILIATIONS

[1]State Key Laboratory for Diagnosis and Treatment of Severe Zoonotic Infectious Diseases, Key Laboratory for Zoonosis Research, Ministry of Education, College of Veterinary Medicine, Jilin University, Changchun, China
[2]Changchun Veterinary Research Institute, Chinese Academy of Agricultural Sciences, Changchun, China
[3]State Key Laboratory of Proteomics, Beijing Proteome Research Center, National Center for Protein Sciences (Beijing), Beijing Institute of Lifeomics, Beijing, China

AUTHOR ORCIDs

Ningyi Jin http://orcid.org/0000-0002-1959-4465
Jian Wang http://orcid.org/0000-0002-8116-7691
Chang Li http://orcid.org/0000-0002-3267-1859

FUNDING

Funder	Grant(s)	Author(s)
Ministry of Science and Technology of the People's Republic of China (MOST)	2021YFD1801103-6	Letian Li
MOST | National Natural Science Foundation of China (NSFC)	31972719	Chang Li
Chinese Academy of Medical Sciences (CAMS)	2020-12M-5-001	Ningyi Jin

AUTHOR CONTRIBUTIONS

Pengfei Hao, Conceptualization, Data curation, Validation, Investigation, Methodology, Writing – original draft | Qiaoqiao Qu, Investigation, Methodology | Letian Li, Funding acquisition, Methodology, Investigation, Project administration | Shouwen Du, Investigation, Methodology | Limin Shang, Software | Chaozhi Jin, Software | Wang Xu, Investigation, Methodology | Zhuo Ha, Investigation, Methodology | Yuhang Jiang, Investigation, Methodology | Jing Chen, Investigation, Methodology | Zihan Gao, Investigation, Methodology | Ningyi Jin, Conceptualization, Supervision, Funding acquisition, Validation, Project administration, Writing – review and editing | Jian Wang, Conceptualization, Data curation, Software, Validation, Writing – review and editing | Chang Li, Conceptualization, Data curation, Supervision, Funding acquisition, Validation, Project administration, Writing – review and editing.

DATA AVAILABILITY

The mass spectrometry proteomics data of proximity labeling have been deposited to iProX with accession number IPX0007242000 and can be accessed through accession number PXD045952 in ProteomeXchange.

REFERENCES

1. Anita A, Pinski AN, Ding S. 2022. Re-examining rotavirus innate immune evasion potential applications of the reverse genetics system. J mBio 13:e0130822. https://doi.org/10.1128/mbio.01308-22
2. Crawford SE, Ramani S, Tate JE, Parashar UD, Svensson L, Hagbom M, Franco MA, Greenberg HB, O'Ryan M, Kang G, Desselberger U, Estes MK. 2017. Rotavirus infection. Nat Rev Dis Primers 3:17083. https://doi.org/10.1038/nrdp.2017.83
3. Arias CF, López S. 2021. Rotavirus cell entry: not so simple after all. Curr Opin Virol 48:42–48. https://doi.org/10.1016/j.coviro.2021.03.011
4. Arias CF, Silva-Ayala D, López S, Tsai B. 2015. Rotavirus entry: a deep journey into the cell with several exits. J Virol 89:890–893. https://doi.org/10.1128/JVI.01787-14
5. Hu L, Crawford SE, Czako R, Cortes-Penfield NW, Smith DF, Le Pendu J, Estes MK, Prasad BVV. 2012. Cell attachment protein VP8* of a human rotavirus specifically interacts with a-type histo-blood group antigen. Nature 485:256–259. https://doi.org/10.1038/nature10996
6. Ciarlet M, Ludert JE, Iturriza-Gómara M, Liprandi F, Gray JJ, Desselberger U, Estes MK. 2002. Initial interaction of rotavirus strains with *N*-acetylneuraminic (sialic) acid residues on the cell surface correlates with VP4 genotype, not species of origin. J Virol 76:4087–4095. https://doi.org/10.1128/jvi.76.8.4087-4095.2002
7. Guerrero CA, Bouyssounade D, Zárate S, Isa P, López T, Espinosa R, Romero P, Méndez E, López S, Arias CF. 2002. Heat shock cognate protein 70 is involved in rotavirus cell entry. J Virol 76:4096–4102. https://doi.org/10.1128/JVI.76.8.4096-4102.2002
8. Guerrero CA, Méndez E, Zárate S, Isa P, López S, Arias CF. 2000. Integrin alpha(V)beta(3) mediates rotavirus cell entry. Proc Natl Acad Sci USA 97:14644–14649. https://doi.org/10.1073/pnas.250299897
9. Londrigan SL, Graham KL, Takada Y, Halasz P, Coulson BS. 2003. Monkey rotavirus binding to alpha2beta1 integrin requires the alpha2 I domain and is facilitated by the homologous beta1 subunit. J Virol 77:9486–9501. https://doi.org/10.1128/JVI.77.17.9486-9501.2003
10. Graham KL, Halasz P, Tan Y, Hewish MJ, Takada Y, Mackow ER, Robinson MK, Coulson BS. 2003. Integrin-using rotaviruses bind alpha2beta1 integrin alpha2 I domain via VP4 DGE sequence and recognize alphaxbeta2 and alphavbeta3 by using VP7 during cell entry. J Virol 77:9969–9978. https://doi.org/10.1128/jvi.77.18.9969-9978.2003
11. Branon TC, Bosch JA, Sanchez AD, Udeshi ND, Svinkina T, Carr SA, Feldman JL, Perrimon N, Ting AY. 2018. Efficient proximity labeling in living cells and organisms with TurboID. Nat Biotechnol 36:880–887. https://doi.org/10.1038/nbt.4201
12. Doerr A. 2018. Proximity labeling with TurboID. Nat Methods 15:764. https://doi.org/10.1038/s41592-018-0158-0
13. Zhang Y, Shang L, Zhang J, Liu Y, Jin C, Zhao Y, Lei X, Wang W, Xiao X, Zhang X, Liu Y, Liu L, Zhuang MW, Mi Q, Tian C, Wang J, He F, Wang PH, Wang J. 2022. An antibody-based proximity labeling map reveals mechanisms of SARS-Cov-2 inhibition of antiviral immunity. Cell Chem Biol 29:5–18. https://doi.org/10.1016/j.chembiol.2021.10.008
14. Wei XF, Fan SY, Wang YW, Li S, Long SY, Gan CY, Li J, Sun YX, Guo L, Wang PY, Yang X, Wang JL, Cui J, Zhang WL, Huang AL, Hu JL. 2022. Identification of STAU1 as a regulator of HBV replication by TurboID-based proximity labeling. iScience 25:104416. https://doi.org/10.1016/j.isci.2022.104416
15. Fang J, Pietzsch C, Witwit H, Tsaprailis G, Crynen G, Cho KF, Ting AY, Bukreyev A, Saphire EO, de la Torre JC. 2022. Proximity Interactome analysis of lassa polymerase reveals eRF3A/GSPT1 as a druggable target for host-directed antivirals. Proc Natl Acad Sci USA 119:e2201208119. https://doi.org/10.1073/pnas.2201208119
16. Rayaprolu S, Bitarafan S, Santiago JV, Betarbet R, Sunna S, Cheng L, Xiao H, Nelson RS, Kumar P, Bagchi P, Duong DM, Goettemoeller AM, Oláh VJ, Rowan M, Levey AI, Wood LB, Seyfried NT, Rangaraju S. 2022. Cell type-specific biotin labeling in vivo resolves regional neuronal and astrocyte proteomic differences in mouse brain. Nat Commun 13:2927. https://doi.org/10.1038/s41467-022-30623-x

17. Kushner J, Papa A, Marx SO. 2021. Use of proximity labeling in cardiovascular research. JACC Basic Transl Sci 6:598–609. https://doi.org/10.1016/j.jacbts.2021.01.005
18. Zhang Y, Song G, Lal NK, Nagalakshmi U, Li Y, Zheng W, Huang P, Branon TC, Ting AY, Walley JW, Dinesh-Kumar SP. 2019. Turboid-based proximity labeling reveals that UBR7 is a regulator of N NLR immune receptor-mediated immunity. Nat Commun 10:3252. https://doi.org/10.1038/s41467-019-11202-z
19. Mair A, Xu S-L, Branon TC, Ting AY, Bergmann DC. 2019. Proximity labeling of protein complexes and cell-type-specific organellar proteomes in arabidopsis enabled by Turboid. Elife 8. https://doi.org/10.7554/eLife.47864
20. Artan M, Barratt S, Flynn SM, Begum F, Skehel M, Nicolas A, de Bono M. 2021. Interactome analysis of caenorhabditis elegans synapses by Turboid-based proximity labeling. Journal of Biological Chemistry 297:101094. https://doi.org/10.1016/j.jbc.2021.101094
21. Zhou LJ, Peng J, Chen M, Yao LJ, Zou WH, He CY, Peng HJ. 2021. *Toxoplasma gondii* SAG1 targeting host cell S100A6 for parasite invasion and host immunity. iScience 24:103514. https://doi.org/10.1016/j.isci.2021.103514
22. Qian P, Wang X, Zhong C-Q, Wang J, Cai M, Nguitragool W, Li J, Cui H, Yuan J. 2022. Inner membrane complex proteomics reveals a palmitoylation regulation critical for intraerythrocytic development of malaria parasite. Elife 11:e77447. https://doi.org/10.7554/eLife.77447
23. Xia LL, He B, Hu TS, Zhang WD, Wang YY, Xu L, Li N, Qiu W, Yu J, Fan QS, Zhang FQ, Tu CC. 2013. Isolation and characterization of rotavirus from bat. Bing Du Xue Bao 29:632–637.
24. Li B, Ding S, Feng N, Mooney N, Ooi YS, Ren L, Diep J, Kelly MR, Yasukawa LL, Patton JT, Yamazaki H, Shirao T, Jackson PK, Greenberg HB. 2017. Drebrin restricts rotavirus entry by inhibiting dynamin-mediated endocytosis. Proc Natl Acad Sci USA 114:E3642–E3651. https://doi.org/10.1073/pnas.1619266114
25. Chen S, Feng C, Fang Y, Zhou X, Xu L, Wang W, Kong X, P Peppelenbosch M, Pan Q, Yin Y. 2019. The eukaryotic translation initiation factor 4F complex restricts rotavirus infection via regulating the expression of Irf1 and Irf7. Int J Mol Sci 20:1580. https://doi.org/10.3390/ijms20071580
26. Rico J, Perez C, Guerrero R, Hernandez J, Guerrero C, Acosta O. 2020. Implication of heat shock proteins in Rotavirus entry into Reh cells. Acta Virol 64:433–450. https://doi.org/10.4149/av_2020_406
27. Green VA, Pelkmans L. 2016. A systems survey of progressive host-cell reorganization during rotavirus infection. Cell Host Microbe 20:107–120. https://doi.org/10.1016/j.chom.2016.06.005
28. He Q, Ren S, Xia Z, Cheng Z, Peng N, Zhu Y, López S. 2018. Fibronectin facilitates enterovirus 71 infection by mediating viral entry. J Virol 92:e02251–02217. https://doi.org/10.1128/JVI.02251-17
29. Ramos I, Stamatakis K, Oeste CL, Pérez-Sala D. 2020. Vimentin as a multifaceted player and potential therapeutic target in viral infections. Int J Mol Sci 21:4675. https://doi.org/10.3390/ijms21134675
30. Suprewicz Ł, Swoger M, Gupta S, Piktel E, Byfield FJ, Iwamoto DV, Germann D, Reszeć J, Marcińczyk N, Carroll RJ, Janmey PA, Schwarz JM, Bucki R, Patteson AE. 2022. Extracellular vimentin as a target against SARS-Cov-2 host cell invasion. Small 18:e2105640. https://doi.org/10.1002/smll.202105640
31. Amraei R, Xia C, Olejnik J, White MR, Napoleon MA, Lotfollahzadeh S, Hauser BM, Schmidt AG, Chitalia V, Mühlberger E, Costello CE, Rahimi N. 2022. Extracellular vimentin is an attachment factor that facilitates SARS-Cov-2 entry into human endothelial cells. Proc Natl Acad Sci USA 119:e2113874119. https://doi.org/10.1073/pnas.2113874119
32. Yu YC, Chien SC, Chen IY, Lai CT, Tsay YG, Chang SC, Chang MF. 2016. Surface vimentin is critical for the cell entry of SARS-Cov. J Biomed Sci 23:14. https://doi.org/10.1186/s12929-016-0234-7
33. Du N, Cong H, Tian H, Zhang H, Zhang W, Song L, Tien P. 2014. Cell surface vimentin is an attachment receptor for Enterovirus 71. J Virol 88:5816–5833. https://doi.org/10.1128/JVI.03826-13
34. Liang JJ, Yu CY, Liao CL, Lin YL. 2011. Vimentin binding is critical for infection by the virulent strain of Japanese encephalitis virus. Cell Microbiol 13:1358–1370. https://doi.org/10.1111/j.1462-5822.2011.01624.x
35. Das S, Ravi V, Desai A. 2011. Japanese encephalitis virus interacts with vimentin to facilitate its entry into porcine kidney cell line. Virus Research 160:404–408. https://doi.org/10.1016/j.virusres.2011.06.001
36. Schäfer G, Graham LM, Lang DM, Blumenthal MJ, Bergant Marušič M, Katz AA. 2017. Vimentin modulates infectious internalization of human papillomavirus 16 pseudovirions. J Virol 91:e00307-17. https://doi.org/10.1128/JVI.00307-17
37. Brunet J-P, Jourdan N, Cotte-Laffitte J, Linxe C, Géniteau-Legendre M, Servin A, Quéro A-M. 2000. Rotavirus infection induces cytoskeleton disorganization in human intestinal epithelial cells: implication of an increase in intracellular calcium concentration. J Virol 74:10801–10806. https://doi.org/10.1128/JVI.74.22.10801-10806.2000
38. Pizarro-Cerdá J, Chorev DS, Geiger B, Cossart P. 2017. The diverse family of Arp2/3 complexes. Trends Cell Biol 27:93–100. https://doi.org/10.1016/j.tcb.2016.08.001
39. Mehedi M, McCarty T, Martin SE, Le Nouën C, Buehler E, Chen Y-C, Smelkinson M, Ganesan S, Fischer ER, Brock LG, Liang B, Munir S, Collins PL, Buchholz UJ. 2016. Actin-related protein 2 (Arp2) and virus-induced filopodia facilitate human respiratory syncytial virus spread. PLoS Pathog 12:e1006062. https://doi.org/10.1371/journal.ppat.1006062
40. Paluck A, Osan J, Hollingsworth L, Talukdar SN, Saegh AA, Mehedi M. 2021. Role of Arp2/3 complex-driven actin polymerization in RSV infection. Pathogens 11:26. https://doi.org/10.3390/pathogens11010026
41. Grikscheit K, Dolnik O, Takamatsu Y, Pereira AR, Becker S. 2020. Ebola virus nucleocapsid-like structures utilize Arp2/3 signaling for intracellular long-distance transport. Cells 9:1728. https://doi.org/10.3390/cells9071728
42. Komano J, Miyauchi K, Matsuda Z, Yamamoto N. 2004. Inhibiting the Arp2/3 complex limits infection of both intracellular mature vaccinia virus and primate lentiviruses. MBoC 15:5197–5207. https://doi.org/10.1091/mbc.e04-04-0279
43. Khasa R, Vaidya A, Vrati S, Kalia M. 2019. Membrane trafficking RNA interference screen identifies a crucial role of the clathrin endocytic pathway and Arp2/3 complex for Japanese encephalitis virus infection in hela cells. J Gen Virol 100:176–186. https://doi.org/10.1099/jgv.0.001182
44. Liu H, Ye G, Liu X, Xue M, Zhou Q, Zhang L, Zhang K, Huang L, Weng C. 2022. Vimentin inhibits type I interferon production by disrupting the Tbk1-IKKε-Irf3 axis. Cell Rep 41:111469. https://doi.org/10.1016/j.celrep.2022.111469
45. He B, Yang F, Yang W, Zhang Y, Feng Y, Zhou J, Xie J, Feng Y, Bao X, Guo H, Li Y, Xia L, Li N, Matthijnssens J, Zhang H, Tu C. 2013. Characterization of a novel G3P[3] rotavirus isolated from a lesser horseshoe bat: a distant relative of feline/canine rotaviruses. J Virol 87:12357–12366. https://doi.org/10.1128/JVI.02013-13
46. He H, Zhou D, Fan W, Fu X, Zhang J, Shen Z, Li J, Li J, Wu Y. 2012. Cyclophilin a inhibits rotavirus replication by facilitating host IFN-I production. Biochem Biophys Res Commun 422:664–669. https://doi.org/10.1016/j.bbrc.2012.05.050
47. Tian Z, Zhang J, He H, Li J, Wu Y, Shen Z. 2017. MiR-525-3p mediates antiviral defense to rotavirus infection by targeting nonstructural protein 1. Biochim Biophys Acta Mol Basis Dis 1863:3212–3225. https://doi.org/10.1016/j.bbadis.2017.09.003
48. Song L, Chen J, Hao P, Jiang Y, Xu W, Li L, Chen S, Gao Z, Jin N, Ren L, Li C. 2022. Differential transcriptomics analysis of IPEC-J2 cells single or coinfected with porcine epidemic diarrhea virus and transmissible gastroenteritis virus. Front. Immunol 13:844657. https://doi.org/10.3389/fimmu.2022.844657
49. Liu Q, Wang H, Zhang H, Sui L, Li L, Xu W, Du S, Hao P, Jiang Y, Chen J, et al. 2022. The global Succinylation of SARS-Cov-2-infected host cells reveals drug targets. Proc Natl Acad Sci USA 119:e2123065119. https://doi.org/10.1073/pnas.2123065119